Princeton Plasma Physics Laboratory

PPPL- 4949

PPPL- 4949

Negative Plasma Potential Relative to Electron-emitting Surfaces

M.D. Campanell

October 2013

PPPL PRINCETON PLASMA PHYSICS LABORATORY

Prepared for the U.S. Department of Energy under Contract DE-AC02-09CH11466.

Princeton Plasma Physics Laboratory
Report Disclaimers

Full Legal Disclaimer

Trademark Disclaimer

PPPL Report Availability

Princeton Plasma Physics Laboratory:

http://www.pppl.gov/techreports.cfm

Office of Scientific and Technical Information (OSTI):

http://www.osti.gov/bridge

Related Links:

U.S. Department of Energy

Office of Scientific and Technical Information

Fusion Links

Negative Plasma Potential Relative to Electron-Emitting Surfaces

M.D. Campanell
Princeton Plasma Physics Laboratory, Princeton University, Princeton, New Jersey 08543, USA

Most works on plasma-wall interaction predict that under strong electron emission, a nonmonotonic "space charge limited" (SCL) sheath forms where plasma potential is positive relative to the wall. We show a fundamentally different sheath structure is possible where the potential monotonically increases towards a positively charged wall that is shielded by a single layer of negative charge. No ion-accelerating presheath exists in the plasma and the ion wall flux is zero. An analytical solution of the "inverse sheath" regime is demonstrated for a general plasma-wall system where the plasma electrons and emitted electrons are Maxwellian with different temperatures. Implications of the inverse sheath effect are (a) the plasma potential is negative, (b) ion sputtering vanishes, (c) no charge is lost at the wall, (d) the electron energy flux is thermal. We predict that the inverse sheath is more likely than the SCL sheath to appear in practice under strong emission. To test the prediction, a plasma bounded by strongly emitting walls is simulated. It is found that inverse sheaths form and ions are confined in the plasma. Our model differs from past PIC simulation studies of emission which contain an artificial source sheath that accelerates ions to the wall.

I. INTRODUCTION

Plasma-wall interaction (PWI) is critical for plasma applications [1]. Bombardment by plasma ions heats the wall and can sputter away wall atoms. Sputtering not only erodes the wall but also contaminates the plasma with unwanted impurities. Bombardment by plasma electrons further heats the wall, increasing the risk of melting. Even in low temperature plasma devices where the walls may not be severely damaged, the PWI is still important; the properties of the plasma itself depend on balances between heating and ionization vs. the losses of energy and charged particles at the walls. The potentials of the walls relative to the plasma and to other walls are important quantities in laboratory and space systems.

For a floating wall, the zero current condition requires the net electron flux to equal the ion flux,

$$\Gamma_{e,net} = \Gamma_p - \Gamma_{emit} = \Gamma_{ion} \quad (1)$$

The plasma electron influx Γ_p is a function of wall potential relative to the plasma Φ. Γ_{ion} is a fixed value independent of Φ by the Bohm criterion [2,3]. Generally $\Gamma_{p0} \equiv \Gamma_p(\Phi=0) >> \Gamma_{ion}$, so when there is no emission, the floating potential Φ_f must be sufficiently negative to reflect away most electrons approaching the wall, satisfying $\Gamma_p(\Phi_f) = \Gamma_{ion}$. The potential profile $\varphi(x)$ takes the form of a monotonic classical Debye sheath, drawn qualitatively in Fig. 1.

Electron emission from the walls can play an important role on PWI. From (1), it is clear that emission forces more plasma electrons to reach the wall to balance Γ_{ion}. Hence emission leads to reduction of $|\Phi_f|$, reduced ion impact energies, enhanced electron energy flux, and cooling of the plasma by the cold emitted electrons. These effects are known to be important in numerous applications including fusion machines [1,4].

A particularly interesting and important question is what happens when a wall emits more electrons than it collects from the plasma. If $\Gamma_{emit} > \Gamma_p$, Eq. (1) cannot be satisfied because Γ_{ion} cannot be negative. This problem can arise when the secondary electron emission (SEE) coefficient of the plasma electrons γ exceeds unity for the wall material; this is known or predicted to occur in certain conditions at surfaces in tokamak scrape-off layers [5,6], plasma thruster channels [7], dusty plasmas [8] and hot astrophysical plasmas [9]. When $\gamma > 1$, $\Gamma_{emit} = \gamma\Gamma_p > \Gamma_p$ for any Φ.

It is also possible to have $\Gamma_{emit} > \Gamma_p$ at surfaces emitting a thermionic or photoelectron current that exceeds the electron saturation current Γ_{p0}, the maximum possible Γ_p. Examples include heated cathodes [10], emissive probes [11] and sunlit objects in space plasmas [9]. In this paper, we will treat the "strong emission problem" in terms of SEE coefficients, though the results apply without loss of generality to other emission types.

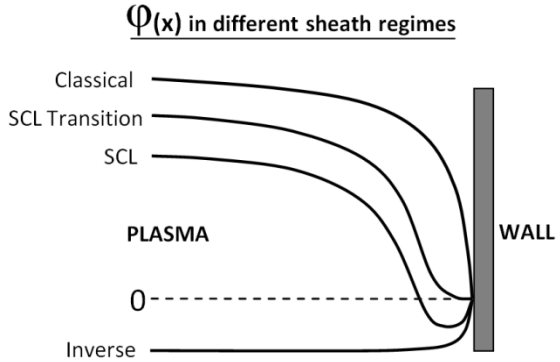

FIG. 1. Qualitative drawings of the potential relative to the wall in the classical (monotonic, Φ_f negative), SCL (nonmonotonic, Φ_f negative) and the inverse (monotonic, Φ_f positive) sheath regimes.

Most papers on PWI with emission predict that when $\gamma > 1$, a "space-charge limited" (SCL) sheath forms [12,13,14,15,16], as illustrated in Fig. 1. In theory, a potential "dip" can reflect enough of the emission back to the wall to maintain zero net current. But we will show that the

"inverse sheath" in Fig. 1 is also possible. The inverse sheath regime has some important features that differ from the familiar classical and SCL regimes. (a) The plasma potential is negative relative to the wall ($\Phi_f > 0$). (b) Ions are confined, so no wall sputtering or loss of charged particles from the plasma occurs. (c) No ion-accelerating presheath structure exists in the plasma interior. (d) The electron influx is the maximum thermal value Γ_{p0}. In light of these features, it worthwhile to investigate the inverse sheath concept in detail.

In Sec. II, we discuss the physical origin of the different sheath structures in Fig. 1 and explain why the inverse sheath was not captured in past theoretical studies of emission. In Sec. III, a mathematical model proving the existence of the inverse sheath solution when $\gamma > 1$ under general conditions is presented. Simple estimates of the potential amplitude and spatial width of the inverse sheath are derived. In Sec. IV, the implications of the inverse sheath effect on PWI are elaborated. In Sec. V, we will provide evidence from theoretical arguments and direct particle simulation that the inverse sheath is more likely to arise in practice than the SCL sheath at strongly emitting walls. Lastly, Sec. VI contains a conclusion summarizing the results.

II. SHEATH STRUCTURE VARIATION WITH EMISSION INTENSITY

A. General Considerations

In this subsection, we will analyze why each sheath structure in Fig. 1 can exist, and under what conditions. The discussion is kept conceptual in order to focus on the physical meaning that is not obvious in mathematical derivations. We will revisit the fundamental assumptions inherent in conventional sheath theories to see why the common assumption of $\Phi_f < 0$ can be violated with emission. Note throughout this paper Φ is defined as φ(wall) - φ(plasma), so it is independent of where the reference point is.

Consider an unmagnetized planar plasma with Maxwellian electrons and cold ions in contact with a non-emitting floating wall. Due to the electron thermal motion it can safely be assumed that in equilibrium, the wall must be negatively charged, and ions will be attracted to the wall. Because the distant plasma must be shielded from the negative wall, the ion density must fall off more slowly than the electron density as the wall is approached, so that the net space charge near the wall is positive. From these assumptions, the Bohm criterion for the ion velocity into the "sheath" is derivable [2,3]. The Bohm criterion essentially fixes Γ_{ion} at the sheath edge, and implies the necessity for a large presheath structure to accelerate ions into the sheath. In equilibrium, Φ_f must be sufficiently negative to maintain $\Gamma_p(\Phi_f) = \Gamma_{ion}$. The exact Φ_f can be calculated, and then the full sheath structure can be derived if desired. The charge density distributions for a non-emitting classical Debye sheath is plotted qualitatively in Fig. 2(a).

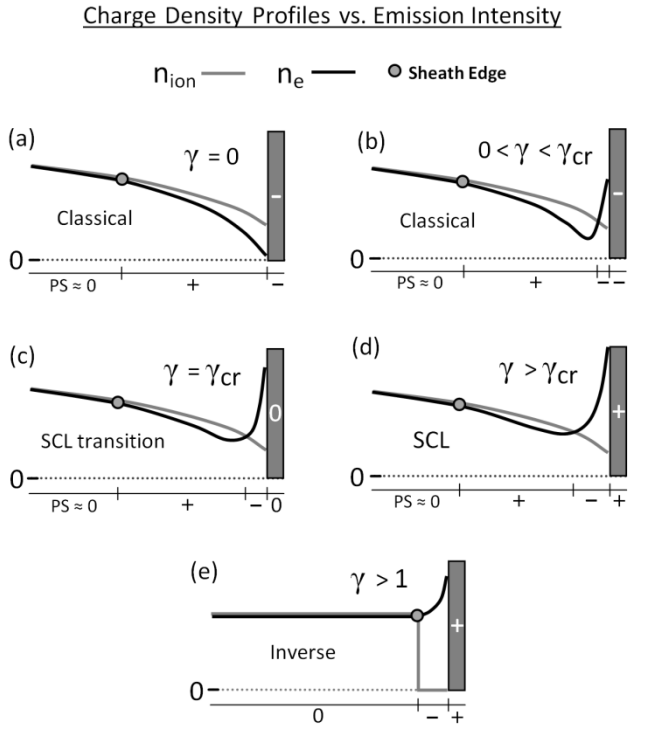

FIG. 2. Qualitative plots of the electron and ion density distributions near the wall for different γ values. The sheath structure corresponding to each charge distribution is indicated (c.f. Fig. 1). "PS" signifies the presheath in (a-d). In (b-d), there are two oppositely charged layers in the sheath. The combined charge of the two layers is positive in (b), zero in (c), and negative in (d).

With electron emission, a few changes occur. For $\gamma > 0$, the floating potential amplitude $|\Phi_f|$ is reduced from the zero current condition $\Gamma_p(\Phi_f) = \Gamma_{ion}/(1-\gamma)$. Emitted electrons contribute to the electron charge density distribution, see Fig. 2(b). The contribution is largest near the wall because emitted electrons start with very small initial velocities and acquire higher velocities further from the wall via sheath acceleration. For small γ, the negative charge layer in the sheath is smaller in magnitude than the positive layer, so the wall charge still must be negative and the potential must increase outward from the wall. Hence the sheath structure remains qualitatively the same as the classical Debye sheath in Fig. 1.

As γ approaches unity, the emission flux increases sharply, $\Gamma_{emit} = \gamma\Gamma_{ion}/(1-\gamma)$. For some critical γ_{cr} below unity, the electron charge in the sheath will equal the ion charge, see Fig. 2(c). At this point the wall charge must be zero for the distant plasma to be shielded. The result is the "transition" sheath in Fig. 1, where the electric field vanishes at the wall. For any further increase in γ, the total charge in the sheath will be negative, Fig. 2(d), so the wall charge must

be positive. Therefore φ(x) is nonmonotonic for $\gamma_{cr} < \gamma < 1$, taking the shape of the SCL sheath in Fig. 1. Although the wall charge is positive in the SCL regime, the *combined* charge of the wall and the negative space charge layer is negative, so a positive charge layer must exist further inward to shield the plasma. This means the same Bohm criterion [2,3] must still be met at the sheath edge, and a presheath must exist to accelerate the ions.

The SCL sheath structure remains a mathematically valid sheath solution for $\gamma > 1$. In the SCL regime, there is an influx of emitted electrons Γ_{ref} that reflect from the potential "dip" and return to the wall. So even if the term $\Gamma_p - \Gamma_{emit} = \Gamma_p(1-\gamma)$ is negative, zero current can be maintained by an SCL sheath if the dip amplitude is sufficient so that,

$$\Gamma_{e,net} = \Gamma_p(1-\gamma) + \Gamma_{ref} = \Gamma_{ion} \tag{2}$$

However note that when $\gamma > 1$, Eq. (2) could be satisfied even with $\Gamma_{ion} = 0$. One could propose that a fundamentally different type of sheath solution should exist where $\Phi_f > 0$, as sketched in Fig. 1. When $\Phi_f > 0$, the ions are confined and the wall draws the full thermal electron influx from the plasma ($\Gamma_p = \Gamma_{p0}$). Some of the emitted electrons will be reflected back to the wall. If Φ_f is sufficiently positive so that $\Gamma_{ref} = \Gamma_{p0}(\gamma-1)$, zero current is maintained. A formal derivation of the inverse sheath structure will be presented in Sec. III. We will find that the charge density profiles appear as sketched in Fig. 2(e).

B. Comparison to Past Theoretical Models of PWI with Emission

The possibility of an emissive plasma sheath with $\Phi_f > 0$ has been unexplored in the literature. It is well known that such a sheath arises at emitting surfaces in vacuum [17], but in plasmas it is widely predicted that $\Phi_f < 0$ for all emission intensities.

Hobbs and Wesson presented the pioneering theoretical treatment of PWI with SEE [12]. They solved Poisson's equation in the sheath using Boltzmann plasma electrons, cold ions and cold emitted electrons. They showed that the electric field at the floating wall drops to zero when γ reaches a critical value γ_{cr} below unity (SCL transition sheath). Other researchers have since considered the influence of the kinetic correction to the EVDF in the sheath [13,16,18], nonzero ion temperature [13], nonzero emitted electron temperature [16], current-carrying surfaces [18], the presence of incident electron beams [19], and supermarginal Mach numbers [15] on emissive sheath structures.

In each of the aforementioned treatments [12,13,15,16,18,19], it is explicit in the model that ions enter the sheath with a (Bohm) flow velocity, and the charge densities are written in terms of a φ(x) that is assumed below the sheath edge potential everywhere in the sheath. The case of $\gamma > 1$ is not derived mathematically because of the complexities inherent in handling a nonmonotonic φ(x); usually the transition sheath with $\gamma = \gamma_{cr}$ is modeled by requiring the electric field to vanish at the wall [12,15,16]. But in most papers it is stated or implied that for all $\gamma > \gamma_{cr}$, a SCL type sheath will form. Hobbs and Wesson wrote "*For $\gamma > \gamma_{cr}$, no monotonic solution for φ(x) exists and a potential well forms such that a fraction of the emitted electrons are returned to the wall in order to maintain the effective γ equal to γ_{cr}. Under these conditions the emission current is space-charge limited*."

Overall, we see that the conventional models of PWI with SEE conclude that a SCL sheath forms under strong emission because it is the only possible solution under the premise of the models. They assume *a priori* that $\Phi_f < 0$ and/or that ions flow to the wall (these assumptions are equivalent as they imply each other). The assumptions are also present in Langmuir's seminal work on cathode sheaths with strong thermionic emission [20]. He stated that emission cannot change Γ_{ion} "for this is fixed by the plasma", and concludes that a nonmonotonic "double sheath" forms under strong emission. Interestingly, a sheath solution where φ(x) monotonically increases from the sheath edge to a strongly emitting wall was claimed in a few PWI models by Sizonenko [21], and by Morozov and Savel'ev [22]. But even in their works, the authors still assumed ions entered the sheath with a substantial flow velocity and reached the wall. A presheath would have to accelerate ions into the sheath for such a structure to exist. The full potential profile must be nonmonotonic and Φ_f must still be negative.

It is the ion flow assumption that can break down under strong emission. As discussed in Sec. II.A, the assumption originates from classical sheath theory without emission, where it can safely be assured that ions flow to the negatively charged wall. The Bohm criterion on the minimum ion flow velocity is a separate subsequent requirement for the formation of the positive shielding charge [2,3]. But with emission, we saw that an ion wall flux only remains necessary for current balance in the range $\gamma < 1$, where the term $\Gamma_p(1-\gamma)$ in (2) is positive, requiring Γ_{ion} to be nonzero. When $\gamma > 1$, because the wall must be positively charged to suppress some of the emission, it is also unnecessary to keep the Bohm criterion because a positively charged wall can be shielded by a *single* layer of negative charge, as in Fig. 2(e). We will find that the $\Phi_f > 0$ sheath solution arises naturally if the ion flow assumption at the sheath edge is removed.

III. – STRUCTURE OF AN INVERSE SHEATH

A. Overview

The result that the inverse sheath potential profile can maintain zero current with $\Gamma_{ion} = 0$ when $\gamma > 1$ by suppressing the "extra emission" seems intuitive. However, showing that the inverse sheath can exist requires proving

that it is self-consistent with the corresponding charge density profiles.

Suppose φ(x) is flat in the neutral plasma interior and starts increasing monotonically from the sheath edge to the wall, as in Fig. 1. Assuming the plasma ions are cold and non-flowing, the ions cannot climb to a higher potential. Therefore, the ion density is zero in the sheath, as in Fig. 2(e). It follows that the charge density will be negative everywhere in the sheath (plasma electrons flow freely to the wall and clearly produce a nonzero density everywhere). Hence from Poisson's equation, φ(x) will monotonically increase from the edge to the wall. If the wall is charged positively to balance the negative charge in the sheath, the plasma interior to the sheath edge will be shielded and φ(x) can indeed be flat in the interior.

We conclude that the requisite charge density profiles can exist self-consistently with the potential profile structure. To more closely investigate properties of the inverse sheath such as its spatial size and potential amplitude, we will present an analytical model.

B. Mathematical model:

Consider an unmagnetized planar plasma contacting a floating wall with a given $\gamma > 1$. Let Φ_{-1} denote the positive wall potential relative to the sheath edge, see Fig 3. Let N designate the neutral plasma density at the edge. Assuming the ions are cold, the ion density N_{ion} drops abruptly from N to zero at the edge, c.f. Fig. 2(e). The electron density N_e in the inverse sheath consists of three distinct components, one corresponding to each flux component in Fig. 3.

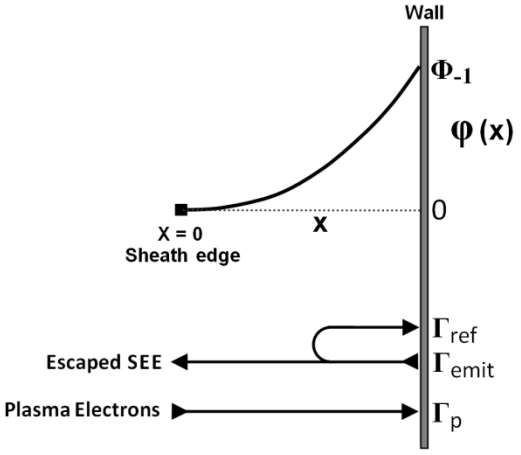

FIG. 3. Parameters and notations used for the analytical inverse sheath model.

Let us assume the thermal plasma electrons approaching the wall have a half-Maxwellian distribution of temperature T_p, starting with density N_P^{SE} at the edge. The plasma electrons accelerate through the inverse sheath towards the wall, producing a density in terms of φ given by,

$$N_P(\varphi) = N_P^{SE} \exp\left(\frac{e\varphi}{T_p}\right) erfc\left(\sqrt{\frac{e\varphi}{T_p}}\right) \tag{3}$$

Suppose the secondaries are emitted with a half-Maxwellian distribution of temperature T_{emit}, starting with a density N_{emit}^{wall} at the wall. The density of secondaries traveling away from the wall under the retarding force is expressible by a Boltzmann factor,

$$N_{emit}(\varphi) = N_{emit}^{wall} \exp\left(\frac{e(\varphi - \Phi_{-1})}{T_{emit}}\right) \tag{4}$$

All secondaries emitted with kinetic energy normal to the wall less than $e\Phi_{-1}$ will be unable to escape the inverse sheath. They will reflect back to the wall. The charge density at each point from reflected secondaries is,

$$N_{ref}(\varphi) = N_{emit}^{wall} \exp\left(\frac{e(\varphi - \Phi_{-1})}{T_{emit}}\right) erf\left(\sqrt{\frac{e\varphi}{T_{emit}}}\right) \tag{5}$$

Eqs. (3)-(5) can be formally derived by solving the Vlasov equation accounting for the cutoffs, and then integrating the distribution functions to get the densities. We omit the details because similar expressions are ubiquitous in sheath theories. For instance, the emitted and reflected secondaries in Eqs. (4) and (5) are respectively analogous to the plasma electrons that decelerate in, and reflect back from, a classical sheath (c.f. Ref. [18]).

So far, N_P^{SE} and N_{emit}^{wall} in (3)-(5) are unspecified quantities which should be expressed in terms of the known N. The condition for neutrality of the plasma must account for the charge density from secondaries that escape the inverse sheath,

$$N_P^{SE} + N_{emit}^{SE} = N \tag{6}$$

The secondary electron density at the edge N_{emit}^{SE} is expressible in terms of N_{emit}^{wall} via (4) with $\varphi = 0$.

$$N_{emit}^{SE} = N_{emit}^{wall} \exp\left(\frac{-e\Phi_{-1}}{T_{emit}}\right) \tag{7}$$

N_{emit}^{wall} and N_P^{SE} can be linked through γ. The plasma electron influx is the full thermal flux of the half-Maxwellian

source, $\Gamma_p = \Gamma_{p0} = N_P^{SE}(T_p / 2m_e\pi)^{1/2}$. The emitted flux from the wall is $\Gamma_{emit} = N_{emit}^{wall}(T_{emit} / 2m_e\pi)^{1/2}$. Then because $\Gamma_{emit} = \gamma\Gamma_{p0}$ (by definition of SEE coefficient) we have,

$$N_{emit}^{wall}\sqrt{\frac{T_{emit}}{2m_e\pi}} = \gamma N_P^{SE}\sqrt{\frac{T_p}{2m_e\pi}} \tag{8}$$

Now to determine Φ_{-1}, we use the zero current condition, $\Gamma_p - \Gamma_{emit} + \Gamma_{ref} = 0$. With $\Gamma_p = \Gamma_{emit}/\gamma$ it follows,

$$\Gamma_{ref} = \frac{\gamma - 1}{\gamma}\Gamma_{emit} \tag{9}$$

In terms of Γ_{emit}, the flux of the half-Maxwellian secondaries that escape past the inverse sheath barrier is $\Gamma_{emit}\exp(-e\Phi_{-1}/T_{emit})$. So Γ_{ref} is just the complement,

$$\Gamma_{ref} = \Gamma_{emit}\left[1 - \exp\left(\frac{-e\Phi_{-1}}{T_{emit}}\right)\right] \tag{10}$$

Equating (9) with (10) yields a simple expression for the inverse sheath amplitude Φ_{-1}.

$$e\Phi_{-1} = T_{emit}\ln\gamma \tag{11}$$

Now plugging (11) into (7) and solving Eqs. (6)-(8) for N_P^{SE} and N_{emit}^{wall} gives,

$$N_P^{SE} = \frac{N}{1 + \sqrt{T_p / T_{emit}}} \tag{12}$$

$$N_{emit}^{wall} = \frac{\gamma N\sqrt{T_p / T_{emit}}}{1 + \sqrt{T_p / T_{emit}}} \tag{13}$$

Summing Eqs. (3)-(5) where Φ_{-1}, N_P^{SE} and N_{emit}^{wall} are defined in (11)-(13) gives the total electron density in the inverse sheath $N_e = N_p + N_{emit} + N_{ref}$ in terms of φ.

C. Discussion and Application of the Model

The exact potential profile solution φ(x) and corresponding $N_e(x)$ for a given {N, T_p, T_{emit}, γ} can be calculated by solving Poisson's equation numerically using the expression for $N_e(\varphi)$ derived above. We will show in this subsection that the essential properties of the inverse sheath can be described in simple terms analytically.

One important property of the inverse sheath is that its amplitude is very small compared to classical and SCL sheaths in hot plasmas. Classical and SCL sheaths always have amplitudes $\geq \sim T_p$. On the other hand, the inverse sheath amplitude $T_{emit}\ln(\gamma)$ is determined by T_{emit} no matter how large T_p is. Although γ itself varies with T_p if the emission type is SEE, the function $\gamma(T_p)$ has a maximum less than 2 for most materials [23]. So in general for SEE, $e\Phi_{-1} < T_{emit}$.

To investigate the electron density, we insert $e\varphi = e\Phi_{-1} = T_{emit}\ln(\gamma)$ into the formula for $N_e(\varphi)$ to give an expression for the total electron density at the wall interface N_e^{wall}. We write N_e^{wall} in terms of the dimensionless $T_R \equiv T_p/T_{emit}$ because only the temperature ratio appears in the expression.

$$N_e^{wall} = N\frac{\gamma^{\frac{1}{T_R}}\,erfc\left(\sqrt{\frac{\ln\gamma}{T_R}}\right) + \gamma\sqrt{T_R}\left[1 + erf\left(\sqrt{\ln\gamma}\right)\right]}{1 + \sqrt{T_R}} \tag{14}$$

In Fig. 4, we plot N_e^{wall} vs. T_R for various γ values. We focus on the range $T_R > 1$ because only this range is of much practical interest. T_{emit} for various emission types is only a few eV or less [16,24]. For plasmas hot enough to induce $\gamma > 1$ from a typical material, T_p is from tens to hundreds of eV [23]. While thermionic or photoemission can induce an inverse sheath in a colder plasma, T_p will still substantially exceed T_{emit} in most conditions.

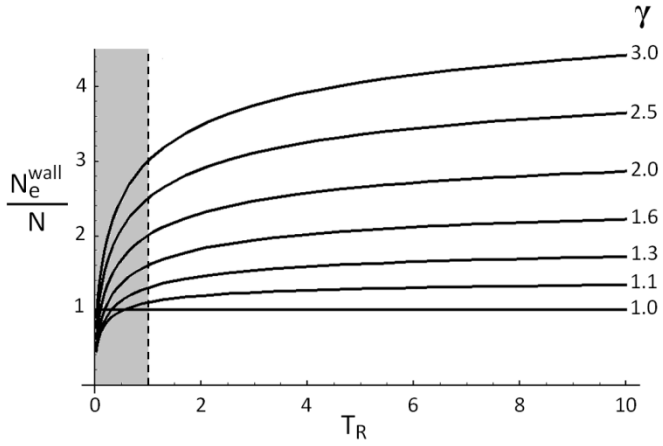

Fig. 4. Variation of N_e^{wall} with γ and $T_R \equiv T_p/T_{emit}$. N_e^{wall} is normalized to the sheath edge plasma density N. The range $T_R < 1$ is unrealistic but is included for completeness.

We see that for $T_R > 1$, the electron density in the inverse sheath increases towards the wall because $N_e^{wall} > N$. While this does not prove that the increase is monotonic, monotonicity can be shown by evaluating $dN_e(\varphi)/d\varphi$ analytically, confrming it is positive for all $T_R > 1$ and using the chain rule $dN_e/dx = dN_e/d\varphi \times d\varphi/dx$. We omit the calculation for brevity.

In Fig. 4, N_e^{wall} increases with γ and with T_R. In the limit of $T_R >> 1$, (14) reduces to,

$$N_e^{wall} = N\gamma\left[1 + erf\left(\sqrt{\ln\gamma}\right)\right] \quad (15)$$

Because usually γ < 2 for SEE [23], and $N_e^{wall} < 2N\gamma$ via (15), this puts an upper bound on N_e in an inverse sheath of ~4N.

A useful approximation of the inverse sheath structure can now be derived. The preceding analysis shows that the electron density in an inverse sheath always exceeds N, but not by more than a factor of a few. Therefore, given that N_{ion} is zero, it is reasonable to approximate the total charge in the inverse sheath as a flat profile, with constant density -N. Poisson's equation in the sheath is then approximately,

$$\frac{d^2\varphi(x)}{dx^2} = \frac{eN}{\varepsilon_0} \quad (16)$$

Setting the origin x = 0, φ = 0 at the sheath edge, assuming zero electric field at the edge, and integrating (16) twice gives a parabolic potential profile,

$$\varphi(x) = \frac{eN}{2\varepsilon_0}x^2 \quad (17)$$

Applying the boundary condition $\varphi(x_{wall}) = \Phi_{-1}$ at the wall, we can determine the location of the wall relative to the sheath edge from (17). This gives a simple estimate of the spatial size of an inverse sheath Δx_{inv},

$$\Delta x_{inv} \approx \sqrt{\frac{2\varepsilon_0 T_{emit}\ln\gamma}{e^2 N}} \quad (18)$$

Eq. (18) is a robust estimate for SEE-driven inverse sheaths. Even if $N_e(x)$ were to increase by a factor of 4 from the sheath edge to the wall, Δx_{inv} from (18) would still be accurate within better than a factor of two. For thermionic emitting surfaces, the equivalent γ can be much larger (e.g. up to 52 in Ref. 10), so that $N_e^{wall} >> N$. An improved estimate for Δx_{inv} is obtainable by using $\frac{1}{2}N_e^{wall}$ instead of N in (18), where N_e^{wall} is calculated from (14).

Another important property of the inverse sheath is that its spatial size is very small. To see this quantitatively, we compare to a common estimate of a non-emitting classical Debye sheath size $\Delta x_D \approx 10\lambda_D$, (see p. 76 of Ref. [1]), where $\lambda_D = (\varepsilon_0 T_p/e^2 N)^{1/2}$ is the Debye length. Dividing Δx_{inv} from (18) by $10\lambda_D$ gives,

$$\frac{\Delta x_{inv}}{\Delta x_D} \approx \sqrt{\frac{T_{emit}\ln\gamma}{50T_p}} \quad (19)$$

So because usually $T_p >> T_{emit}$, and because of the $(50)^{1/2}$ factor, it follows $\Delta x_{inv} << \Delta x_D$. We conclude that the inverse sheath arising when γ > 1 is far smaller than the classical sheath that would arise if the same plasma (same N and T_p) were facing a non-emitting material (γ = 0). The inverse sheath is also far smaller than the SCL sheath that could arise in theory for the same γ > 1. (The structure of the ion-rich part of the SCL sheath is similar to that of the non-emitting sheath, so it has a similar size scale.)

As a final comment we can test the accuracy of the equations from this inverse sheath model by checking limits. As γ → 1 from above, N_e^{wall} → N in (14), Φ_{-1} → 0 in (11), and Δx_{inv} → 0 in (18), as should be expected because no sheath structure is needed if γ = 1 exactly. For γ < 1, the inverse sheath solution should break down. Indeed with γ < 1, N_e^{wall} and Δx_{inv} are undefined, and $\Phi_{-1} < 0$ in (11), contradicting the requirement that the wall potential exceeds the sheath edge potential.

D. Effect of nonzero ion temperature

The main reason for using $T_{ion} = 0$ in the model was for simplicity, and to show that the ions do not need to reach the wall when γ > 1. For nonzero T_{ion}, the inverse sheath solution still always exists when γ > 1. The key fundamental concept is that ions do not need to enter the sheath with a *flow velocity*. When there is no flow velocity at the inverse sheath edge, $N_{ion}(\varphi)$ decreases with increasing φ as the wall is approached. So because the electron density increases with increasing φ (Sec. III.C), the charge between the edge and the wall is automatically negative. Hence the argument of Sec. III.A that the inverse sheath solution exists self-consistently is valid for nonzero T_{ion}.

The mathematical model can be extended to account for thermal ions. Thermal ions will enter and reflect from an inverse sheath in the same way that thermal plasma electrons behave in a classical sheath. When $T_{ion} << T_{emit}$, the influence of ions is negligible, and the cold ion approximation is valid. For larger T_{ion}, the ions produce a significant charge density in the inverse sheath, which will cause the sheath spatial size to increase by a modest amount over the estimate of (18).

Nonzero T_{ion} will also produce a nonzero Γ_{ion}. This will cause Φ_{-1} to increase, but only by a small amount. If the ions approaching the wall are half-Maxwellian at the sheath edge, the flux in terms of Φ_{-1} is,

$$\Gamma_{ion} = \frac{N\sqrt{\frac{T_{ion}}{2m_{ion}\pi}}\exp\left(\frac{-e\Phi_{-1}}{T_{ion}}\right)}{1 + erf\left(\sqrt{\frac{e\Phi_{-1}}{T_{ion}}}\right)} \quad (20)$$

In (20), it was assumed that the *total* ion density at the sheath edge is N. So the denominator gives the fraction of ions

approaching the wall, accounting for wall losses and the return of ions reflected in the sheath. Now if Γ_{ion} is included in the zero current condition (9) it can be shown that the (transcendental) solution for Φ_{-1} becomes,

$$e\Phi_{-1} = T_{emit}\left[\ln\gamma + \ln\left(\frac{1+\dfrac{\sqrt{\dfrac{T_{ion}}{T_{emit}}}\sqrt{\dfrac{m_e}{m_{ion}}}\exp\left(\dfrac{-e\Phi_{-1}}{T_{ion}}\right)}{1+erf\left(\sqrt{\dfrac{e\Phi_{-1}}{T_{ion}}}\right)}}{1-\dfrac{\sqrt{\dfrac{T_{ion}}{T_{p}}}\sqrt{\dfrac{m_e}{m_{ion}}}\exp\left(\dfrac{-e\Phi_{-1}}{T_{ion}}\right)}{1+erf\left(\sqrt{\dfrac{e\Phi_{-1}}{T_{ion}}}\right)}}\right)\right] \quad (21)$$

The second term in the right hand side of (21) is a positive term appearing due to the nonzero T_{ion}. But because of the smallness of m_e/m_{ion} ($< 10^{-3}$), it follows that the argument of the logarithm is very close to unity for most realistic values of T_{ion}/T_{emit} and T_{ion}/T_p. (The unknown factors exp() and 1/(1+erf()) serve to further push the argument closer to unity). Overall, we see the thermal ions will not increase Φ_{-1} significantly compared to the $T_{ion} = 0$ solution unless γ is also very close to unity.

IV. – IMPLICATIONS OF THE INVERSE SHEATH EFFECT

The sheath physics for strongly emitting surfaces is relevant to a diverse variety of systems such as those mentioned in the introduction. The inverse sheath would have important implications on the PWI because it is fundamentally different in several ways from classical and SCL sheaths (which we will collectively refer to as "$\Phi_f < 0$ sheaths").

One important aspect of the inverse sheath regime is that the ion-induced sputtering is negligible. This could be significant in many systems, particularly fusion machines. It has long been proposed that deliberate use of emitting wall materials could benefit future tokamaks such as ITER [25], the basis being that emission reduces the amplitude of classical sheaths, thereby reducing the impact energy of ions. The phenomenon of space charge saturation was thought to limit the possible benefit of the emission, as $|\Phi_f|$ was assumed to never fall below the SCL limit [25]. However, in light of the inverse sheath effect, it should be possible to fully eliminate ion sputtering because Γ_{ion} drops to zero. While Γ_{ion} will not be negligible if the ions are hot, the sputtering will still be dramatically reduced because there is no ion acceleration to the wall. Even with $T_{ion} > 0$, both the flux of ions and their impact energies are always much smaller in the inverse sheath regime compared to the $\Phi_f < 0$ regimes.

Another key consequence of $\Gamma_{ion} = 0$ is that the wall is no longer a plasma sink. In general, the state of a plasma depends crucially on the balance between the ion-electron generation and losses. In the $\Phi_f < 0$ regimes, the loss rate of charged particles to the boundaries is a fixed value (essentially independent of γ) determined by the Bohm velocity and plasma density at the sheath edge. But for $\gamma > 1$ in the inverse sheath regime, the loss rate of ions and electrons to the boundaries is zero. No neutrals will recycle back to the plasma from the walls. Although there will be some charge loss if $T_{ion} > 0$, the loss rate is always much smaller in the inverse sheath regime compared to the $\Phi_f < 0$ regimes.

A possible drawback of the inverse sheath regime is that the electron influx to the wall is very large. A sheath with $\Phi_f < 0$ serves to insulate a wall by reflecting away many plasma electrons. Authors have stated that the SCL regime is "considered the maximum plasma interaction of ambient plasmas with the surrounding boundary [15]" because Γ_p is assumed to never exceed its value at space charge saturation. But all electrons are unconfined in the inverse sheath regime. This is unfortunate in terms of wall heating because the wall faces the full thermal electron influx. Nonetheless the inverse sheath regime is not worse than the SCL regime considering the extra energy flux from plasma electron impact is offset by the elimination of the ion energy flux.

The difference between $\Phi_f > 0$ and $\Phi_f < 0$ is significant in any case where the surface potentials are important. For example, when emissive probes are used to measure space potential in plasmas, it is usually assumed that the sheath is SCL. The space potential is taken to be $\sim 1T_p$ above the measured floating potential of the probe [11]. But if the PWI is in the inverse sheath regime, the space potential will fall below the measured floating probe potential, by a small margin $\sim T_{emit}$. While this would make no practical difference in the measurement if only the potential differences between points in an isothermal plasma are sought, there are other situations where the absolute potentials of surfaces relative to each other are important, such as for differentially charged spacecraft. Strong emission is possible for spacecraft that are in contact with hot background plasmas and/or intense sunlight [9].

Although we treated floating walls formally in Sec. III, we want to briefly point out how the inverse sheath effect is also relevant to current-carrying walls. When a plasma is bounded between mutually biased walls, the plasma potential itself is determined self-consistently by the condition that the total current out of the plasma is zero globally. If the walls emit sufficiently strong electron currents, then the wall potentials can all exceed the plasma potential. For instance, consider a planar plasma between two conducting walls biased to equal potentials (that is, both walls have the same Φ relative to the plasma). Let one wall emit a flux Γ_{emit} and the other wall be non-emitting. For $\Gamma_{emit} = 0$, the walls have some

$\Phi < 0$. For larger Γ_{emit}, Φ becomes less negative. For some critical Γ_{emit}, the emitting wall sheath becomes SCL. General theories may assume that the walls remain at $\Phi < 0$ for arbitrarily large Γ_{emit} as the additional emission is limited by the virtual cathode [20]. However, there will be a critical Γ_{emit} beyond which both walls can have $\Phi > 0$. The total current between the walls will still be limited but not in the same physical way.

V. – WHICH SHEATH STRUCTURE WILL APPEAR IN PRACTICE UNDER STRONG EMISSION?

A. Theoretical Considerations

Both the SCL sheath and inverse sheath are legitimate theoretical solutions to the strong emission problem. Because the two regimes have drastically different properties as discussed in Sec. IV, it is instinctive to ask which sheath will appear in practice at floating surfaces.

One argument favoring the inverse sheath is that it is a simpler structure; a positive wall charge is shielded by an equal negative charge layer facing the wall (Fig. 2(e)). The SCL sheath configuration is complicated. It has four pieces; a positive wall charge, a negative charge layer in front of the wall larger than the wall charge, a neutralizing positive charge further inward, and an ion-accelerating presheath (Fig. 2(d)). Another argument is to consider a thought experiment where an initially neutral wall is placed in a plasma. At t=0, the wall charging rate is $d\sigma/dt = -e\Gamma_{p0}(1-\gamma)$. Thus when $\gamma > 1$, the material initially charges positively, so ions will immediately be repelled away from the wall, rather than drawn to it. The long term evolution should lead to an inverse sheath.

It might appear more plausible for a SCL sheath to exist at a wall with $\gamma > 1$ if γ was initially below unity, and then increased past unity. For instance, a wall contacting a plasma that increases in temperature can undergo such a transition. An analogy for thermionic emission is an emissive probe is inserted into a plasma and then turned on. In these cases, because a SCL sheath with a presheath and a dip would already exist before γ crossed unity, it could remain after the transition. But this does not guarantee that a SCL sheath would persist indefinitely. The inverse sheath is probably the more stable configuration considering it is more natural for ions to be repelled from a positively charged wall than drawn to it. In addition, experiments have shown that potential dips are spontaneously destroyed due to the eventual accumulation of slow ions produced by i-n collisions or by charge exchange with slow neutrals [10].

B. Past Empirical Studies

Because theoretical arguments alone cannot determine which sheath will form under strong emission, direct empirical proof would be valuable. Unfortunately, probing the full structure of the space potential in sheaths is difficult due to their small spatial size, and resolving the much smaller negative electric field region near the wall in an emissive sheath is formidable. So there are few high resolution probe measurements of the space potential near emitting surfaces in the literature.

Intrator *et al.* published space potential measurements near a floating thermionic emitting cathode [10]. In Fig. 6 of the paper, it was found when the emission was very strong, the cathode floated more positively than the background plasma by about 2V, as in an inverse sheath regime. But the potential profile was also nonmonotonic with a dip qualitatively similar to a SCL sheath. So it is difficult to categorize the result. We suggest that the nonmonotonic properties could be due to the presence of an ion beam; in their apparatus, the plasma was produced in a source region, and flowed into the cathode region through a pair of mutually biased grids. Because of this setup, ions were launched towards the cathode with energy ~3eV. Ion beams can significantly alter sheath structures because the current balance and charge density profiles are altered compared to a plasma with non-drifting ions. The ion beam seems to be affecting the profiles because in Fig. 6 of Ref. [10] even $\varphi(x)$ for the same cathode without emission was nonmonotonic, in contrast to how a classical non-emitting sheath usually looks.

Measurement of a virtual cathode dip structure near an emitting surface was also claimed recently by Li *et al.* [26]. But it was not a strongly emitting floating surface that we wish to study here. In their paper, the surface was electrically biased below the plasma potential, and the virtual cathode formation was reportedly due to ion-induced SEE. Emitted fluxes from ion-induced SEE should never be large enough to exceed the plasma electron saturation current.

Another way one can empirically study sheath physics with emission is by particle-in-cell (PIC) simulation. Simulation allows direct non-invasive measurement of potential profiles and tracking of the emitted electrons, so that the PWI can be analyzed closely.

In most PIC simulation studies of PWI, a plasma is produced at a "source" boundary in front of the "collector" (wall) [13,14,27,28]. Ions and electrons are injected into the plasma domain at the same rate to maintain global neutrality. Because the ions and electrons have different velocity distributions, a non-neutral charge distribution forms near the source, creating a potential drop called a "source sheath". The source sheath is not caused by PWI at the collector, which could be arbitrarily far from the source. But the source sheath accelerates ions towards the collector, so that the true plasma source facing the collector has drifting ions. This type of setup can artificially distort the physics of the $\gamma > 1$ problem because it forces ions to flow to the wall.

Schwager presented the seminal simulation-based study of PWI with electron emission [13]. In Fig. 9 of the paper, a SCL collector sheath with a "dip" was observed in a simulation with $\gamma = 1.5$. But in the same potential profile near the source boundary was an ion-accelerating source sheath of

amplitude ~30 times larger than the dip. More recently Zhang *et al.* simulated PWI with strong emission to investigate interesting sheath oscillation behavior [29]. In the simulation the ions were modeled as a spatially uniform background density flowing to the wall at a fixed velocity set to the Bohm velocity.

Overall, it is not yet known empirically what the sheath structure looks like at strongly emitting floating surfaces where ions are not directed towards the surface by an external mechanism (i.e. a mechanism other than the PWI). So here we will simulate a full bounded plasma system where the charged particles, and their temperatures, are sustained naturally within the plasma itself, and no ion beams are produced. That way ions will flow to the walls if and only if they "need" to.

C. Simulation of a full scale plasma bounded by walls with $\gamma > 1$

As a simple yet realistic system, we will simulate a bounded planar plasma with a uniform background E×B field, see Fig. 5(a). A planar system is ideal for our study because the surface geometry will not affect the sheath physics. The E×B background field will serve as a natural heating mechanism for the plasma; it does not (directly) affect the sheath physics either because it does not alter particle velocities normal to the walls. An electrostatic direct implicit particle-in-cell code for this configuration was produced by D. Sydorenko [30]. It has been applied for modeling PPPL Hall thruster (HT) plasmas [31,32]. The simulation results have provided valuable insight into the experimental measurements discussed in a recent review paper by Raitses *et al.*, see Ref. [33].

A theoretical analysis of the plasma properties and the wall fluxes as a function of the controllable simulation parameters is given in Ref. 32 for applications to HT's. However, the theory assumes $\Phi_f < 0$ sheaths always exist at the walls. When the electron E×B drift energy exceeds a threshold value, the electrons incident on the walls eject more than one secondary on average ($\gamma > 1$). The system enters the inverse sheath regime, where the physics behind the plasma properties and the PWI drastically changes. A detailed theoretical explanation of the transition between the two regimes is given in Ref [34]. But in Fig. 1 of Ref. [34], the inverse sheath structure was unclear. The simulation spatial grid, which was suitable for resolving classical Debye sheaths, could not resolve the much smaller inverse sheath. The ~1V amplitude inverse sheath was also obscured by strong potential fluctuations caused by plasma waves.

Here in Fig. 5 a new simulation with enhanced grid resolution and time-averaged data is presented in order to reveal the true steady state sheath physics. The discharge behaves basically as follows. Secondaries are emitted from the walls with a low energy thermal distribution. The secondaries that overcome the inverse sheath propagate across the plasma in the x-direction while undergoing E×B drift motion in the y-z plane. With E_z = 300V/cm and B_x =100G, the drift energy oscillates between 0 and 102eV. So the electrons carry high energies upon impact at the other wall, sufficient to induce a net SEE coefficient of 1.3 from the boron nitride ceramics material. Particle collisions are included in the model but their effects are negligible here. With a (xenon) plasma density $n_p = 1.8 \times 10^{17}$ m^{-3} and a (uniform) neutral background density $n_n = 10^{18}$ m^{-3}, it turns out the transit time of the unconfined electrons from wall to wall is less than the average time between collisions of all types. (On the other hand when E_z/B_x is lower, classical sheaths confine most electrons in the plasma interior. In that case the neutral, Coulomb and turbulent collisions are crucial to the plasma properties, as explained in Ref. [32].)

Fig. 5 shows the profiles of $\varphi(x)$, $N_e(x)$, $N_{ion}(x)$ and $V_{x,ion}(x)$ over the plasma domain. The plasma width was set to 1mm so that the plasma and sheath regions can be resolved with a reasonable computation time. There are 229 grid points spaced uniformly 4.4μm apart. The plotted profiles are averages of 17 snapshots taken 25ns apart in order filter out fluctuations from plasma waves and instabilities that appear in the simulations [34] (periodic and random fluctuations average out to zero long term).

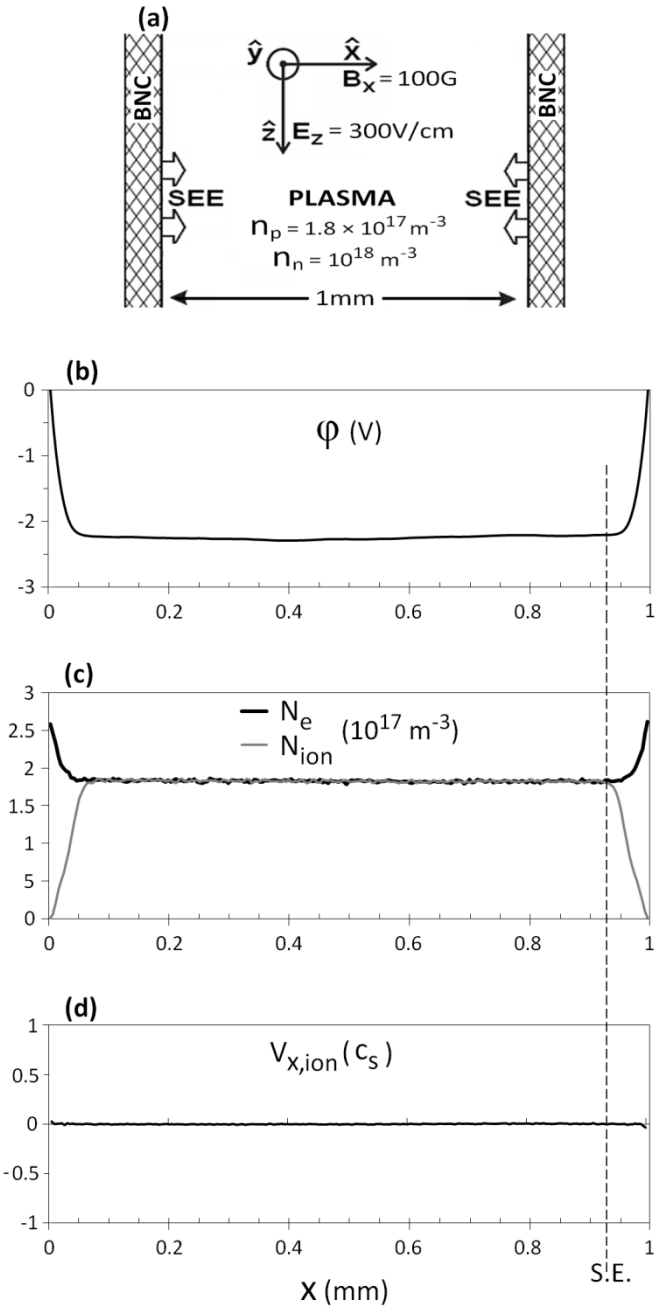

FIG. 5. (a) Schematic of the simulation model with the main discharge parameters for the current run listed. (b) The electrostatic potential relative to the right wall. (c) Charge density profiles. (d) Ion velocity normal to the walls. $V_{x,ion}(x)$ is the mean velocity of the ions in the two cells neighboring each grid point, normalized to c_s = 2053m/s, the ion sound speed calculated from the EVDF in the simulation. Note the plots are high resolution; the grid spacing 4.4μm is more than 10 times smaller than the sheath size.

D. Analysis of the Simulation Results

Usually for a plasma between two walls [1], $N_e(x)$ and $N_{ion}(x)$ decrease by a factor of about two from the plasma center to the sheath edges because of the presheaths. There is a substantial ion flow velocity throughout the plasma domain; $V_{x,ion}(x)$ increases from zero at the plasma center, to ~c_s (ion sound speed) at the sheath edges. The potential φ(x) is positive relative to the wall everywhere between the two sheath edges, and is curved due to the presheath gradient. These presheath features should remain present with secondary emission under the conventional assumption that Φ_f is negative for all emission intensities. The features are indeed observed for simulations with $\gamma < 1$ using the same simulation configuration [32].

But the profiles in Fig. 5 sharply differ from conventional PWI. There is clearly no ion-accelerating presheath structure in the system. $N_e(x)$ and $N_{ion}(x)$ are flat between the two sheath edges. The ion mean velocity $V_{x,ion}(x)$ is negligible everywhere compared to c_s. The sheath regions consist not of a double charge layer but instead a single negative charge layer. From the sheath edges towards the wall, $N_e(x)$ and φ(x) monotonically increase, and $N_{ion}(x)$ monotonically decreases. The potential φ(x) is negative and flat between the sheaths. Overall, the properties of the profiles match the characteristics of the inverse sheath regime predicted theoretically in this paper.

The inverse sheath's spatial width is 68 μm. This value is within a factor of two of the estimate $(2\varepsilon_0\Phi_{-1}/eN)^{1/2}$ = 37 μm from (18) based on the flat charge density profile approximation. (We used Φ_{-1} = 2.2V and $N = 1.8 \times 10^{17}\ m^{-3}$.) The underestimate is attributable to finite ion temperature. In this run the ions are (almost) Maxwellian with T_{ion} = 0.5eV, so they can penetrate a significant distance into the inverse sheaths, though very few can reach the wall as exp(-0.5/2.2) = 0.01.

The value Φ_{-1} = 2.2V cannot be calculated easily in terms of simulation parameters. First, the coefficient γ =1.3 was not a set parameter but is determined self-consistently with the irregular plasma EVDF and wall SEE yield function. Also, the emission EVDF in the model is complicated. The "true secondaries" are emitted with an energy distribution $\sim w^{1/2}\exp(-w/T_{emit})$ and have a non-isotropic angular distribution [30]. We set T_{emit} to 5eV (to make the inverse sheath larger and easier to resolve, while 2eV is a more realistic value). There are also "non-true" secondaries consisting of hot electrons that reflect or backscatter off the wall. The higher energy secondaries is the main reason $e\Phi_{-1}$ exceeds the estimate $T_{emit}\ln\gamma = 5eV\times\ln1.3 = 1.3$ eV based on the Maxwellian emission EVDF calculation.

The author has conducted studies of the sheath structures in this simulation model as the parameters (E, B, and other conditions) are varied over a wide range. It turns out whenever $\gamma > 1$, inverse sheaths form at the walls. While it should also be possible for a SCL sheath to form, a SCL sheath has not yet been observed in steady state. So it seems the inverse sheath is the more natural solution, at least in this simulation configuration.

Interestingly, a nonmonotonic φ(x) qualitatively similar to a SCL sheath does appear in some simulations, as shown

in Fig. 3 of Ref. [35] by Sydorenko *et al*.. However, it only exists briefly during an instability. It was later shown that the nonmonotonic $\varphi(x)$ appears because a classical sheath with a presheath exists initially, and then the "weakly confined electron" instability causes the wall charge to change from negative to positive before the heavy ions have a chance to respond, (see Fig. 5 of Ref. [36] and the discussion therein). Hence the nonmonotonic $\varphi(x)$ is not a true SCL sheath as the corresponding charge density profiles cannot exist in steady state.

VI. - CONCLUSION

A new type of sheath structure that can appear in plasma systems with surfaces emitting strong secondary, thermionic or photon-induced electron currents was introduced. Past theoretical models predicting that a nonmonotonic SCL sheath with positive plasma potential forms when $\gamma > 1$ rely on an assumption that ions always have to flow to the wall [12,13,14,15]. But when the emission exceeds a threshold value, the zero current condition and the plasma shielding requirement can be maintained without ion flow to the wall. Relaxing the ion flow assumption at the sheath edge allows the new "inverse sheath" solution.

In the inverse sheath regime, the potential $\varphi(x)$ is flat in the plasma up to the sheath edge, and monotonically increases from the edge to a positively charged wall. Ions are repelled from the wall and the ion velocity is zero everywhere in the plasma. An analytical inverse sheath solution was derived for a general plasma-wall system where the plasma electrons and emitted electrons are Maxwellian with temperatures T_p and T_{emit}. The inverse sheath amplitude $e\Phi_{-1} = T_{emit}\ln\gamma$ and its spatial width, estimated as $\Delta x_{inv} = (2\varepsilon_0 T_{emit}\ln\gamma/e^2N)^{1/2}$ are much smaller than a classical Debye sheath.

The author believes the inverse sheath regime is more likely to appear in practice than the SCL sheath. Theoretically, considering the wall must be positively charged in both regimes, it would seem more natural for ions to be repelled from a positively charged wall than drawn to it. For some concrete evidence, a PIC simulation a Hall discharge at high voltage where the SEE coefficient exceeded unity at the walls was presented. Inverse sheaths formed at the walls. Ions were indeed confined and there was zero ion flow throughout the plasma domain. Although a PIC simulation study by another researcher reported formation of a SCL sheath at an emitting wall [13], the model had an artificial "source sheath" that accelerated ions to the wall.

The inverse sheath effect drastically alters how the plasma interacts with a wall. Most importantly, with zero ion flux, the sputtering and charged particle loss to the wall are eliminated. No presheath potential gradient exists to accelerate the ions. The distributions of potential, ion density and electron density in the sheath and the plasma are much different in the inverse sheath regime compared to the classical and SCL regimes. The author hopes these results motivate future experimental studies of the sheath structure facing strongly emitting surfaces.

[1] P.C. Stangeby, *The Plasma Boundary of Magnetic Fusion Devices*, Plasma Physics Series (IOP, Bristol, 2000).
[2] R.H. Cohen and D.D. Ryutov, Contrib. Plasma Phys. **44**, 111 (2004).
[3] K.U. Riemann, J. Phys. D **24**, 493 (1991).
[4] I.V. Tsvetkov and T. Tanabe, J. Nucl. Mater. **266**, 714 (1999).
[5] R.A. Pitts and G.F. Matthews, J. Nucl. Mater. **176**, 877 (1990).
[6] J.P. Gunn, Plasma Phys. Control. Fusion **54**, 085007 (2012).
[7] Y. Raitses, D. Staack, A. Smirnov and N.J. Fisch, Phys. Plasmas **12**, 073507 (2005).
[8] J. Pavlů, J. Šafránovká, Z. Němeček, and I. Richterová, Contrib. Plasma Phys. **49**, 169 (2009).
[9] E.C. Whipple, Rep. Prog. Phys. **44**, 1197 (1981).
[10] T. Intrator, M.H. Cho, E.Y. Wang, N. Hershkowitz, D. Diebold and J. DeKock, J. Appl. Phys. **64**, 2927 (1988).
[11] J.P. Sheehan, Y. Raitses, N. Hershkowitz, I. Kaganovich and N.J. Fisch, Phys. Plasmas **18**, 073501 (2011).
[12] G.D. Hobbs and J.A. Wesson, Plasma Phys. **9**, 85 (1967).
[13] L.A. Schwager, Phys. Fluids B **5**, 631 (1993).
[14] F. Taccogna, S. Longo and M. Capitelli, Phys. Plasmas **11**, 1220 (2004).
[15] J. Seon, E. Lee, W. Choe and H.J. Lee, Curr. Appl. Phys. **12**, 663 (2012).
[16] J.P. Sheehan *et. al.*, in International Conference on Plasma Science, Edinburgh, UK, 2012.
[17] A. Dove, M. Horanyi, X. Wang, M. Piquette, A.R. Poppe and S. Robertson, Phys. Plasmas **19**, 043502 (2012).
[18] C.A. Ordonez, Phys. Fluids B **4**, 778 (1992).
[19] T. Gyergyek, J. Kovačič and M. Čerček, Phys. Plasmas **17**, 083504 (2010).
[20] I. Langmuir, Phys. Rev. **33**, 954 (1929).
[21] V.L. Sizonenko, Sov. Phys. Tech. Phys. **26**, 1345 (1981).
[22] A.I. Morozov and V.V. Savel'ev, Plasma Phys. Rep. **33**, 20 (2007).
[23] C.A. Ordonez and R.E. Peterkin, J. Appl. Phys. **79**, 2270 (1996).
[24] M. Kaminsky, Atomic and ionic impact phenomena on metal surfaces (Academic Press, New York, 1965).
[25] M.J. Embrechts and D. Steiner, Proceedings of IEEE 13th Symposium on Fusion Engineering **1**, 538 (1989).
[26] W. Li, J.X. Ma, J. Li, Y. Zheng and M. Tan, Phys. Plasmas **19**, 030704 (2012).
[27] A. Bergmann, Nucl. Fusion **42**, 1162 (2002).
[28] D. Tskhakaya and S. Kuhn, Contrib. Plasma Phys. **40**, 484 (2000).
[29] F. Zhang, D. Yu, Y. Ding and H. Li, Appl. Phys. Lett. **98**, 111501 (2011).
[30] D. Sydorenko, Ph.D. thesis, U. of Saskatchewan, 2006.
[31] D. Sydorenko, *et al.*, Phys. Plasmas **13**, 014501 (2006).
[32] I.D. Kaganovich, Y. Raitses, D. Sydorenko and A. Smolyakov, Phys. Plasmas **14**, 057104 (2007).
[33] Y. Raitses *et al.*, IEEE Trans. Plasma Science, **39**, 4, (2011).
[34] M.D. Campanell, A.V. Khrabrov and I.D. Kaganovich, Phys. Rev. Lett. **108**, 255001 (2012).
[35] D. Sydorenko, I. Kaganovich, Y. Raitses and A. Smolyakov, Phys. Rev. Lett. **103**, 14 (2009).
[36] M.D. Campanell, A.V. Khrabrov and I.D. Kaganovich, Phys. Plasmas **19**, 123513 (2012).

The Princeton Plasma Physics Laboratory is operated
by Princeton University under contract
with the U.S. Department of Energy.

Information Services
Princeton Plasma Physics Laboratory
P.O. Box 451
Princeton, NJ 08543

Phone: 609-243-2245
Fax: 609-243-2751
e-mail: pppl_info@pppl.gov
Internet Address: http://www.pppl.gov